Science of the Total Environment 630 (2018) 1628–1640

Contents lists available at ScienceDirect

Science of the Total Environment

journal homepage: www.elsevier.com/locate/scitotenv

Carbon burial and storage in tropical salt marshes under the influence of sea level rise

A.C. Ruiz-Fernández [a,*], V. Carnero-Bravo [b], J.A. Sanchez-Cabeza [c], L.H. Pérez-Bernal [a], O.A. Amaya-Monterrosa [d], S. Bojórquez-Sánchez [e], P.G. López-Mendoza [b], J.G. Cardoso-Mohedano [f], R.B. Dunbar [g], D.A. Mucciarone [g], A.J. Marmolejo-Rodríguez [h]

[a] Unidad Académica Mazatlán, Instituto de Ciencias del Mar y Limnología, Universidad Nacional Autónoma de México, Calz. J. Montes Camarena s/n, Playa Sur, 82040 Mazatlán, Mexico
[b] Posgrado en Ciencias del Mar y Limnología, Universidad Nacional Autónoma de México, Ciudad Universitaria, 04510 Ciudad de México, Mexico
[c] Unidad Académica Procesos Oceánicos y Costeros, Instituto de Ciencias del Mar y Limnología, Universidad Nacional Autónoma de México, Ciudad Universitaria, 04510 Ciudad de México, Mexico
[d] Laboratorio de Toxinas Marinas LABTOX-UES, Universidad de El Salvador, Facultad de Ciencias Naturales y Matemáticas, Final de Av. Mártires y Héroes del 30 julio, San Salvador, El Salvador
[e] Universidad Politécnica de Sinaloa (UPSIN), Carretera municipal libre Mazatlán-Higueras Km 3, Col. Genaro Estrada, CP 82199 Mazatlán, Mexico
[f] CONACYT – Estación el Carmen, Instituto de Ciencias del Mar y Limnología, Universidad Nacional Autónoma de México, Carr. Carmen-Puerto Real km. 9.5, 24157 Ciudad del Carmen, Mexico
[g] Earth System Science, Stanford University, Stanford, CA 94305, USA
[h] Centro Interdisciplinario de Ciencias Marinas, Instituto Politécnico Nacional, Av. Instituto Politécnico Nacional s/n, Playa Palo de Sta. Rita, 23096 La Paz, Mexico

HIGHLIGHTS

- ^{210}Pb-dated sediment cores from tropical saltmarshes showed marine transgression.
- C_{org} concentration, stock and burial varied widely within and among study sites.
- C_{org} stocks in tropical saltmarshes are as high as in other blue carbon ecosystems.
- Marine transgression caused lower C_{org} sediment concentrations and stocks.
- Sea level rise effects on C_{org} burial rates are masked by other global change impacts.

GRAPHICAL ABSTRACT

ARTICLE INFO

Article history:
Received 22 October 2017
Received in revised form 19 February 2018
Accepted 19 February 2018
Available online xxxx

Editor: D. Barcelo

Keywords:
C_{org} burial rate
C_{org} stock
Tropical salt marsh

ABSTRACT

Coastal vegetated habitats can be important sinks of organic carbon (C_{org}) and mitigate global warming by sequestering significant quantities of atmospheric CO_2 and storing sedimentary C_{org} for long periods, although their C_{org} burial and storage capacity may be affected by on-going sea level rise and human intervention. Geochemical data from published ^{210}Pb-dated sediment cores, collected from low-energy microtidal coastal wetlands in El Salvador (Jiquilisco Bay) and in Mexico (Salada Lagoon; Estero de Urias Lagoon; Sian Ka'an Biosphere Reserve) were revisited to assess temporal changes (within the last 100 years) of C_{org} concentrations, storage and burial rates in tropical salt marshes under the influence of sea level rise and contrasting anthropization degree. Grain size distribution was used to identify hydrodynamic changes, and $\delta^{13}C$ to distinguish terrigenous sediments from those accumulated under the influence of marine transgression. Although the accretion rate ranges in all sediment records were comparable, C_{org} concentrations (0.2–30%), stocks (30–465 Mg ha^{-1}, by extrapolation to 1 m depth), and burial rates (3–378 g m^{-2} year^{-1}) varied widely within and

* Corresponding author.
E-mail addresses: caro@ola.icmyl.unam.mx (A.C. Ruiz-Fernández), vladislavc@gmail.com (V. Carnero-Bravo), jasanchez@cmarl.unam.mx (J.A. Sanchez-Cabeza), lbernal@ola.icmyl.unam.mx (L.H. Pérez-Bernal), oscar.amaya@ues.edu.sv (O.A. Amaya-Monterrosa), sara_bojorquez29@hotmail.com (S. Bojórquez-Sánchez), pergualome@gmail.com (P.G. López-Mendoza), jgcardosomo@conacyt.mx (J.G. Cardoso-Mohedano), dunbar@stanford.edu (R.B. Dunbar), dam1@stanford.edu (D.A. Mucciarone).

https://doi.org/10.1016/j.scitotenv.2018.02.246

Sea level rise
Blue carbon

among the study areas. However, in most sites sea level rise decreased C_{org} concentrations and stocks in sediments, but increased C_{org} burial rates. Lower C_{org} concentrations were attributed to the input of reworked marine particles, which contribute with a lower amount of C_{org} than terrigenous sediments; whereas higher C_{org} burial rates were driven by higher mass accumulation rates, influenced by increased flooding and human interventions in the surroundings. C_{org} accumulation and long-term preservation in tropical salt marshes can be as high as in mangrove or temperate salt marsh areas and, besides the reduction of C_{org} stocks by ongoing sea level rise, the disturbance of the long-term buried C_{org} inventories might cause high CO_2 releases, for which they must be protected as a part of climate change mitigation efforts.

1. Introduction

Coastal ecosystems such as tidal wetlands and seagrasses (collectively known as coastal blue carbon ecosystems) are recognized for their capacity to remove CO_2 from the atmosphere and incorporate it, along with trapped plant materials, into their sediments (Howard et al., 2014). Tidal wetlands are important in climate change research because of their sensitivity to sea-level rise and their ability to sequester CO_2 from the atmosphere, which might otherwise contribute to global warming. The capacity of long-term organic carbon burial by wetland sediments primarily depends on the ratio between inputs (organic matter produced *in situ* and *ex situ*) and outputs (decomposition and erosion; Scholz, 2010). Oxygen penetrates and is depleted by aerobic respiration within the upper few millimeters of soil, whereas anaerobic metabolism, especially sulfate reduction, dominates at greater depths (Alongi and Brinkman, 2011). Since this process is less efficient than surface aerobic metabolism, organic carbon is stored almost indefinitely until exposed by shoreline erosion or soil desiccation.

Organic carbon (C_{org}) storage in coastal wetlands can be significantly disturbed by anthropogenic interventions and/or by climate-induced factors, such as increasing air and water temperatures (associated with atmospheric CO_2 increase), change in precipitation patterns, and sea level rise (Smoak et al., 2013). Sea level is perhaps the most urgent concern for intertidal ecosystems as, to persist, their surface elevations must increase in keeping with rising sea level (Chmura et al., 2003). Otherwise, the C_{org} sink capacity of these ecosystems may be compromised, since the buried organic matter may become exposed to conditions favorable to decomposition and remineralization to gaseous form (Breithaupt et al., 2012).

Tropical salt marshes are usually found along semi-sheltered low-energy coastlines, located behind the mangrove fringe, in the highest possible topographic position within the tidal range, so they are intermittently flooded by medium to high tides, at least once fortnightly. High evaporation and relatively infrequent flooding favor the formation of hypersaline soils that can be colonized by halophyte glasswort vegetation (e.g. *Batis maritima*, *Salicornia pacifica*) that can tolerate inundation with sea water and high soil salinity (Costa et al., 2009; Flores-Verdugo et al., 2007). The ecosystem services associated to salt marshes includes fish production, carbon storage and coastal protection; however, they have been historically perceived as wastelands, and have thus experienced intense human impacts (e.g. land reclamation for agriculture, urban development, salt production, waste disposal, livestock grazing, and shrimp aquaculture) for which 25% to 50% of their global historical coverage has been lost (Mcowen et al., 2017 and references therein). These ecosystems are so under-valued that there are no statistics on their extent or loss rate due to anthropogenic transformation in Mexico or El Salvador.

Since 2013, the United Nations Framework Convention on Climate Change established the need to promote sustainable management and conservation of greenhouse gases sinks and reservoirs, including coastal ecosystems. Nowadays, there is an increasing interest to better understand the role of natural coastal wetlands (particularly mangroves, seagrasses and tidal marshes) as long-term carbon sinks, and their role in climate-change mitigation (Howard et al., 2017). However, few quantitative data on C_{org} accumulation and preservation in tropical tidal marshes are available. In addition, despite the efforts to predict the effects of sea level rise on coastal carbon sinks by using numerical models, short term C_{org} degradation experiments, or salinity gradients as analogue for marine transgression (e.g. Kirwan and Mudd, 2012; Van de Broek et al., 2016; Whittle and Gallego-Sala, 2016) this issue is still not clear, mostly owing to the scarcity of field studies that show temporal changes in both ongoing sea level rise and C_{org} accumulation.

With the goal to contribute to the knowledge of the long-term organic carbon burial capacity and carbon storage of tropical salt marshes, and to the discussion on how sea level rise might affect these ecosystem services, published geochemical data from ^{210}Pb-dated sediment cores, collected from four low-energy microtidal tropical salt marsh areas (three from Mexico and one from El Salvador) where marine transgression has been confirmed, were revisited to assess the temporal changes C_{org} concentrations (%), C_{org} stocks (Mg ha^{-1}, stored within 1 m depth and within a centennial scale), and C_{org} burial rates (g m^{-2} year^{-1}). This work provides quantitative information on the long-term C_{org} burial and storage in tropical salt marshes, derived from the retrospective evaluation of C_{org} accumulation in four different geographical areas under the influence of ongoing sea level rise (as shown by geochemical proxies for marine transgression, such as C:N ratios and isotopic organic carbon composition). Our field observations highlight the contribution of tropical salt marshes to CO_2 sequestration and sustain the importance of their preservation to mitigate global warming.

2. Study sites

The Jiquilisco Bay Complex is a Ramsar site and UNESCO biosphere reserve in SE El Salvador (Fig. 1). It has the largest expanse of perennial wetlands in the country, with large areas (~18,700 ha) of mangrove forests which include *Rhizophora mangle*, *R. racemosa*, *R. harrisonii*, *Avicennia germinans*, *A. bicolor*, *Conocarpus erectus*, and *Laguncularia racemosa*, as well as the freshwater mangrove *Bravaisia integerrima*. The main economic activities in this study site are fishing, shellfish extraction, aquiculture, salt extraction, cattle ranching and coconut plantations. The climate is tropical savanna, with a mean annual temperature of 28 °C and a maximum of 36 °C. Annual rainfall ranges from 1600 to 2000 mm, mainly from May to October, and mean annual evapotranspiration is 1944 mm (MARN/AECI, 2004). Most of El Salvador territory is covered by volcanic rock; the stratigraphic succession in the study area consists of Quaternary alluvial deposits covering volcanic strata (Holocene–Pleistocene) of basaltic, andesitic, and dacitic composition (MARN, 2013).

The Estero de Urias Lagoon is an anthropized coastal lagoon at the entrance of the Gulf of California, partially surrounded by the city of Mazatlan (Fig. 1). It is a shallow (~12 m maximum depth) and narrow (<1 km width) inner-shelf barrier-type lagoon (total surface ~ 18 km^2). A combination of permanent seawater exchange and seasonal freshwater supply through runoff yields a salinity range of 25.8–38.4 (Cardoso-Mohedano et al., 2015). The upper lagoon (distal from

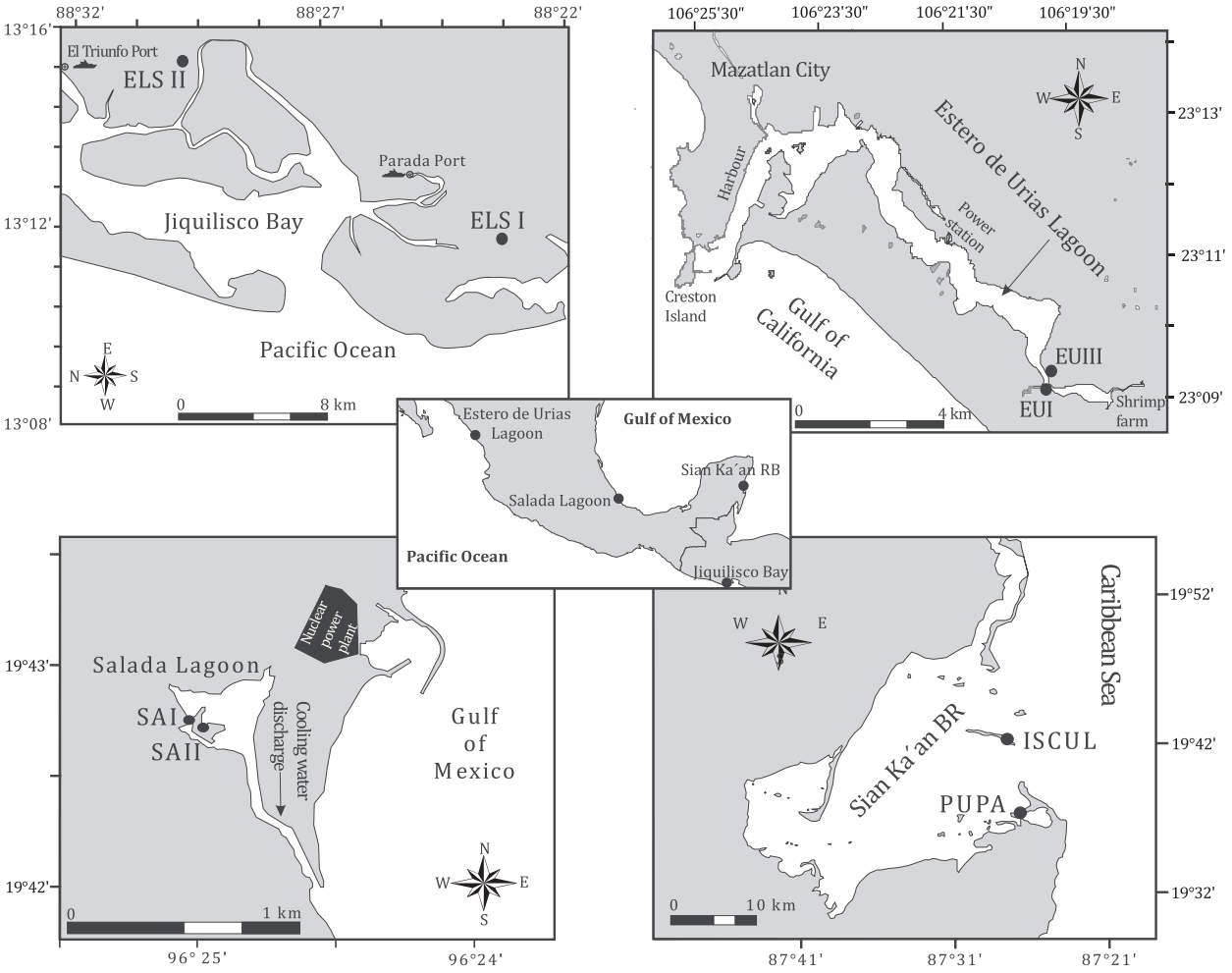

Fig. 1. Location of sampling stations in tropical salt marsh areas in Jiquilisco Bay (ELSI: 13° 12′ 7.6″ N, 88° 23′ 15.75″ W; ELSII: 13° 15′ 3.85″ N, 88° 29′ 59.12″ W); Estero de Urias Lagoon (EU I: 23° 09′ 11.2″ N, 106° 19′ 49.2″ W; EU III: 23° 09′ 19.3″ N, 106° 19′ 40.25″ W); Salada Lagoon (SAI 19° 42′ 47.2″ N, 96° 24′ 47.8″ W; SAII 19° 42′ 45.1″ N, 96° 24′ 42.0″ W); and Sian Ka'an Biosphere Reserve (BR) (ISCUL: 19° 41′ 39.6″ N, 87° 27′ 37.7″ W; and PUPA: 19° 36′ 09.3″ N, 87° 27′ 15.6″ W).

the sea) is surrounded by a mangrove forest colonized by *R. mangle*, *L. racemosa* and *A. germinans*. The climate is warm and humid with average temperature of 25 °C (7.5 °C to 39 °C; SMN, 2014) and summer rains (annual precipitation 700–1300 mm; INEGI, 2009). The coastal plain is composed of Quaternary alluvial soils (predominantly regosol) overlying Tertiary igneous rocks, e.g. andesite, rhyolite, dacite, trachyte, rhyodacite, basalt and tuff (Alba-Cornejo et al., 1979).

The Salada Lagoon is a small (51 ha) and shallow (≤3 m depth) costal lagoon in the state of Veracruz (Gulf of Mexico, Fig. 1), near the Laguna Verde Nuclear Power Plant. The lagoon does not have a permanent freshwater supply (except rainfall runoff), and until the mid-1970s its connection with the sea was limited, which caused desiccation owing to high evaporation rates and, consequently, high salinities (up to 70; Rodríguez Castañeda, 1994). Nowadays, the lagoon receives the discharge of cooling waters from the power plant through a channel built in 1981 (Morales-Lozano, 2011). The channel established a permanent connection between the lagoon and the sea, decreasing salinities to values comparable to seawater (37; Rodríguez Castañeda, 1994). The climate is warm-humid with summer rains and an average annual temperature that ranges from 21 °C to 28 °C (CONABIO, 2012). The mangrove species present are *R. mangle*, *L. racemosa* and *A. germinans*. The area is characterized by the presence of igneous extrusive rocks, e.g. andesite, basalt, basic tuff and breccia; with phaeozem and vertisol as the main soil types.

Sian Ka'an is a large (~528,000 ha) and complex hydrological system on the Mexican Caribbean coast, registered as a World Heritage Site, UNESCO Biosphere Reserve, Wildlife Protection Area and RAMSAR site. It lies on a partially emerged coastal karstic plain facing a 120 km-long barrier reef, and includes two large shallow bays surrounded by mangroves (*R. mangle*, *A. germinans* and *L. racemosa*), numerous sinkholes ("cenotes") and a vast extension of tropical deciduous forests. Much of the Reserve is limestone of Pleistocene origin. The climate is tropical with summer rains (mean annual rainfall 1300 mm) and occasional cyclones, with a mean annual temperature of 26.5 °C (extreme values ranging from 4.5 °C to 40.5 °C).

3. Methods

Most sediment records referred here have already been used to describe environmental processes related to global change (Amaya-Monterrosa et al., 2014; Ruiz-Fernández et al., 2016; Carnero-Bravo et al., 2016; Bojórquez-Sánchez et al., 2017), where further methodological details can be found.

3.1. Sampling

Sediment push cores were collected with PVC tubes (10 cm diameter, 50 cm length) between May 2012 and April 2013 (Fig. 1). The cores

were cut into 1 cm thick sections, and samples were freeze-dried and ground to powder in a porcelain mortar (except those for grain size analysis). The sediment cores were collected in remote areas, far away from human and cattle access, in relatively flat sites with presence of glassworts (*S. pacifica* and/or *B. maritima*), between 10 and 50 m behind the landward edge of mangrove areas. The shorter distance between the closest tidal creek and the sampling sites in Jiquilisco Bay (El Salvador) were 560 m for core ELS I and 270 m for core ELS II; and in Mexico, 100 m for EU I and 150 m for EUIII (Estero de Urias Lagoon); 320 m for SA I and 150 m for SA II (Salada Lagoon); and 50 m for ISCUL and 10 m for PUPA (Sian Ka'an Biosphere Reserve).

3.2. Laboratory analysis

Grain size distribution (sand, silt and clay fractions, %) was determined by laser diffraction with a Malvern Mastersizer 2000. The elemental concentrations and isotopic composition of organic C and N were determined on carbonate-free sediment samples, using elemental

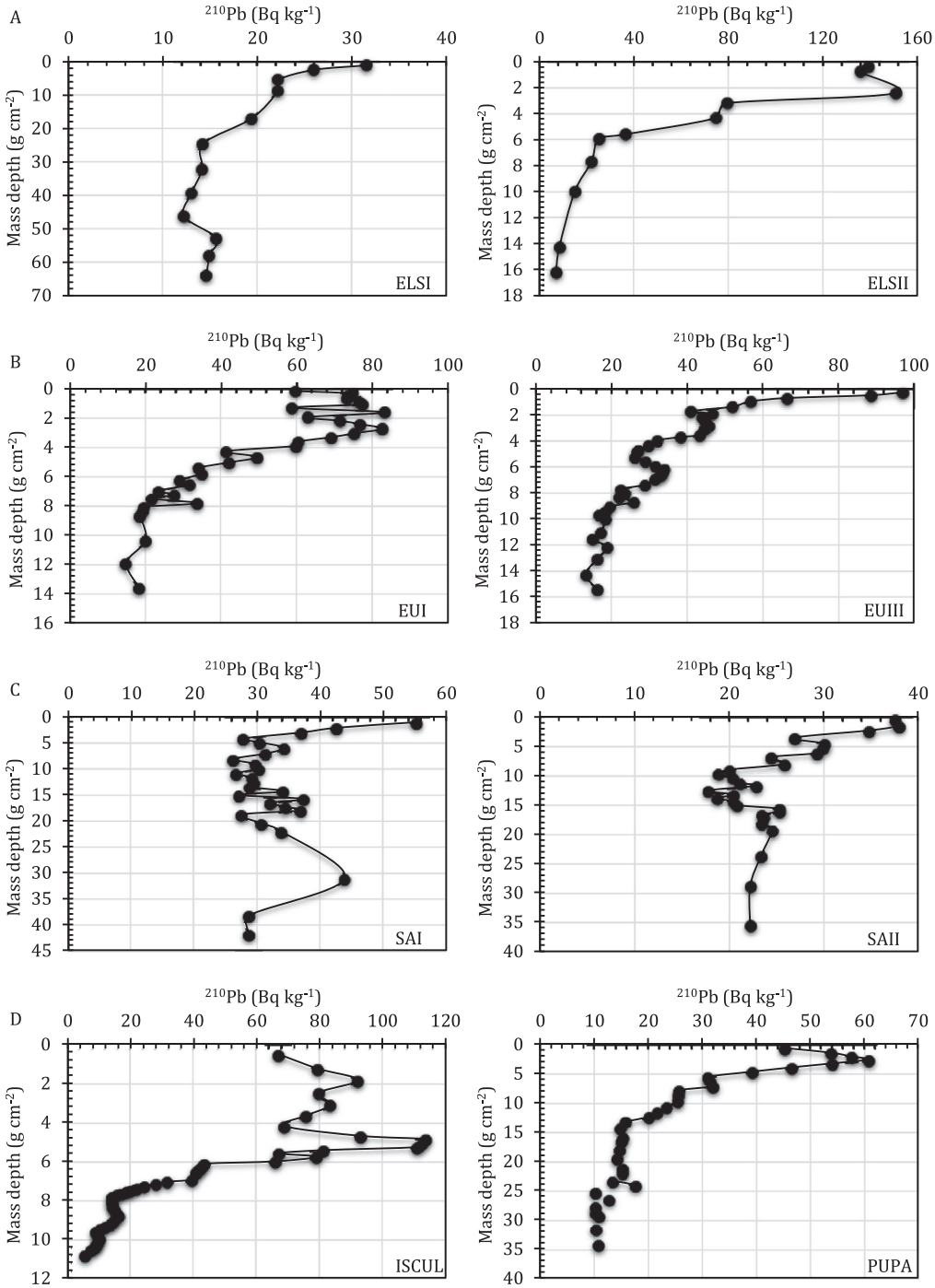

Fig. 2. Total ^{210}Pb activity depth profiles from tropical salt marshes in El Salvador (A = ELSI I, ELSI II, Jiquilisco Bay) and Mexico (B = EUI, EUIII, Estero de Urias Lagoon; C = SAI, SAII, Salada Lagoon; and D = ISCUL, PUPA, Sian Ka'an BR).
Modified from Amaya-Monterrosa et al. (2014), Ruiz-Fernández et al. (2016), Carnero-Bravo et al. (2016), and Bojórquez-Sánchez et al. (2017).

analysers coupled to isotope ratio mass spectrometers. At Stanford University Stable Isotope Laboratory (cores from Estero de Urias Lagoon and Jiquilisco Bay) sediments were placed into silver capsules and decarbonated with 6% H_2SO_4, whereas at CICIMAR (cores from Salada Lagoon) and GEOTOP-UQAM (cores from Sian Ka'an Biosphere Reserve) sediments were treated with 1 M HCl and freeze dried before analysis. Isotopic results are presented in standard delta notation (‰), with $\delta^{13}C$ reported relative to the Vienna Pee Dee Belemnite (VPDB) carbonate standard and $\delta^{15}N$ relative to air.

Total ^{210}Pb (^{210}Pb) activities were determined through its radioactive descendant ^{210}Po by alpha spectrometry (Ortec Ametek 576A spectrometer), by the method described by Ruiz-Fernández and Hillaire-Marcel (2009), whereas supported ^{210}Pb ($^{210}Pb_{sup}$) activities were determined through the measurement of ^{226}Ra by low background gamma-spectrometry in well-type HPGe detectors (ORTEC). Excess ^{210}Pb ($^{210}Pb_{xs}$) was calculated as the difference between ^{210}Pb and $^{210}Pb_{sup}$. The ^{210}Pb-derived chronologies were calculated with the constant flux (CF) model (Robbins, 1978) which assumes a constant flux of ^{210}Pb to the sediments, and variable accumulation rates (the assumptions and formulae for dating, mass accumulation rates (MAR) and sediment accretion rates (SAR), are described in detail in Sanchez-Cabeza and Ruiz-Fernández, 2012). Age, MAR and SAR uncertainties were estimated by Monte Carlo simulation with 30,000 iterations, by using the ^{210}Pb dating Excel workbook described in Sanchez-Cabeza et al. (2014). The ^{210}Pb-derived dating data is available as Supplementary information.

Analytical quality control included accuracy assessment through the analysis of reference materials, and precision assessment by replicate analysis of a single sample ($n = 6$). Results were within the reported range of the certified values. The variation coefficients were <5% for grain size distribution, <3% for C and N isotopic composition, and <10% for ^{210}Pb activities.

3.3. Data analysis

In order to evaluate the influence of sea level rise on C_{org} accumulation, a correlation analysis between C_{org} concentrations and $\delta^{13}C$ (as a proxy for marine transgression) was performed. All data was used as a single data set; normality of the data distribution was tested by the Kolmogorov-Smirnov test ($p < 0.01$) and the statistical significance of the correlation analysis was determined by using a Student's *t*-test ($p < 0.05$).

4. Results

4.1. ^{210}Pb activity profiles and ^{210}Pb-derived mass accumulation rates

The ^{210}Pb profiles for all the analyzed cores are collated in Fig. 2 from previously published work (Amaya-Monterrosa et al., 2014; Ruiz-Fernández et al., 2016; Carnero-Bravo et al., 2016; Bojórquez-Sánchez et al., 2017). All sediment records spanned at least 100 years. The ranges of both mass accumulation rate (MAR, 0.03 ± 0.01 to 0.88 ± 0.65 g cm^{-2} year^{-1}) and sediment accretion rates (SAR, 0.04 ± 0.01 to 1.03 ± 0.77 cm year^{-1}) were comparable among the sediment cores (Table 1).

SAR ranges were compatible with those reported for mangrove areas in (a) the Gulf of Mexico (0.24 cm year^{-1} in Terminos Lagoon, Lynch et al., 1989; 0.2–0.4 cm year^{-1} in the lagoons of Terminos, Chelem and Celestun, in the Western Yucatan Peninsula, Gonneea et al., 2004); (b) the Marismas Nacionales System in the Pacific coast of Mexico (0.08 ± 0.01 to 0.36 ± 0.02 cm year^{-1}; Ruiz-Fernández et al., 2018); (c) the global estimate of 0.25–0.36 cm year^{-1} by Twilley et al. (1992); and (d) the general mangrove forest worldwide range of 0.5–0.7 cm year^{-1} by Alongi (2012).

The estimated recent rates of sea level rise (mm year^{-1}, derived from sediment accretion rates, under the assumption that these ecosystems accrete at a similar rate to sea level rise) are comparable across the four study sites, ranging from 3.4 ± 0.5 to 3.7 ± 0.3 in Jiquilisco (period 2010–2013, Amaya-Monterrosa et al., 2014), 2.8 ± 0.1 to 3.9 ± 0.1 in Estero de Urias Lagoon (1990–2012, Ruiz-Fernández et al., 2016), 3.0 ± 0.7 to 4.5 ± 0.6 in Sian Ka'an BR (2010–2013, Carnero-Bravo et al., 2016), and 1.7 ± 0.2 to 4.3 ± 0.3 in Laguna Salada (2007–2013, Bojórquez-Sánchez et al., 2017). These results are comparable to the mean sea level rise rate recorded at the nearest tide gauge of each study site, for the available periods. They are also compatible with the mean sea level rise trends estimated from tide gauges in Mexico and El Salvador (CO-OPS, 2013; no uncertainties provided) and the global mean SLR of 3.0 ± 0.7 mm year^{-1} from the analysis of sea-level data of a global network of tide gauges (from 1993 to 2010, Hay et al., 2015). Despite that sea level rise rates derived from SAR reflect local (relative) sea level rise trends, our estimations are also compatible with the global mean sea level rise (GMSL) of 3.4 ± 0.4 mm year^{-1} derived from multi-mission satellite altimetry data (1993–2014; Ablain et al., 2017 and references therein). It should be noticed that altimetry-derived GMSL indicates the general state of sea level across the oceans and not at any specific location, and that the accuracy of

Table 1
Accumulation rates and geochemical characteristics of sediment cores from tropical salt marshes in El Salvador and Mexico. See Fig. 1 for location of sampling stations.

		MAR (g cm^{-2} year^{-1})	SAR (cm year^{-1})	Clay (%)	Silt (%)	Sand (%)	N (%)	C_{org} (%)	$\delta^{13}C$ (10^{-3})	$\delta^{15}N$ (10^{-3})	C:N	C_{org} burial (g m^{-2} year^{-1})
ELS I	Min	0.17 ± 0.16	0.12 ± 0.09	2.2	16.2	58.7	0.01	0.2	−25.21	NA	10.5	3.5 ± 3.3
	Max	0.52 ± 0.10	0.38 ± 0.08	4.5	36.9	81.5	0.05	0.5	−21.43	NA	21.8	16.9 ± 2.6
ELS II	Min	0.07 ± 0.01	0.16 ± 0.02	2.6	26.8	0.0	0.26	5.6	−26.97	1.37	15.9	97.2 ± 14.6
	Max	0.15 ± 0.01	0.40 ± 0.05	16.8	88.2	70.7	1.27	17.3	−26.12	1.93	45.6	254.8 ± 22.8
EU I	Min	0.03 ± 0.01	0.09 ± 0.02	1.8	56.6	0.0	0.32	6.7	−26.00	3.89	13.7	22.4 ± 5.8
	Max	0.20 ± 0.02	0.65 ± 0.09	23.8	93.1	30.1	0.70	14.0	−24.10	6.20	37.6	158.4 ± 20.6
EU III	Min	0.03 ± 0.01	0.07 ± 0.01	4.4	46.5	0.0	0.34	9.2	−26.35	2.36	10.2	28.3 ± 5.9
	Max	0.15 ± 0.02	0.36 ± 0.01	17.6	93.1	46.1	1.72	16.8	−20.30	7.51	40.6	234.1 ± 57.0
SA I	Min	0.04 ± 0.01	0.04 ± 0.01	3.9	21.4	14.8	0.02	0.2	−21.72	−4.62	14.0	3.1 ± 0.9
	Max	0.88 ± 0.65	1.03 ± 0.77	16.4	71.7	74.7	0.10	1.9	−17.76	2.70	43.7	69.0 ± 46.1
SA II	Min	0.03 ± 0.01	0.06 ± 0.01	1.8	8.4	14.0	0.03	0.6	−22.86	−0.56	14.5	9.9 ± 2.1
	Max	0.38 ± 0.13	0.54 ± 0.18	19.4	70.4	89.8	0.29	3.6	−15.19	3.48	30.3	94.2 ± 8.0
ISCUL	Min	0.06 ± 0.00	0.07 ± 0.01	9.9	49.2	14.5	0.37	3.3	−26.53	NA	10.2	46.7 ± 5.8
	Max	0.28 ± 0.03	0.45 ± 0.06	15.7	71.3	40.8	1.83	30.3	−16.66	NA	30.9	378.0 ± 33.8
PUPA	Min	0.03 ± 0.01	0.04 ± 0.01	4.7	21.1	45.2	0.07	0.7	−25.37	NA	9.0	2.8 ± 0.9
	Max	0.24 ± 0.03	0.30 ± 0.07	12.1	45.1	73.2	0.16	3.1	−18.43	NA	28.2	19.3 ± 3.9
Total	Min	0.03 ± 0.01	0.04 ± 0.01	1.8	8.4	0.0	0.01	0.2	−26.97	−4.62	9.0	2.8 ± 0.9
	Max	0.88 ± 0.65	1.03 ± 0.77	23.8	93.1	89.8	1.83	30.3	−15.19	7.51	45.6	378.0 ± 33.8

MAR = mass accumulation rate; SAR = sediment accretion rate; NA = not available. C_{org} burial is the product of C_{org} (%) and MAR (g cm^{-2} year^{-1}). MAR, SAR and C_{org} burial rates correspond to the past ~100 years. ELS I and ELS II corresponds to Jiquilisco Bay (El Salvador); EU I and EU III to Estero de Urias Lagoon, SA I and SA II to Salada Lagoon, and ISCUL and PUPA to Sian Ka'an BR (Mexico).

the altimetry-derived GMSL values is affected by the possibility of altimeter drifts, changes of satellite missions, and the geophysical corrections needed, for which satellite altimetry is less sensitive to long term (decadal) variability than tide-gauge measurements (Nerem et al., 2018). Nonetheless, tide gauge data in our study sites is very limited, and for this reason SAR-derived sea level rise trends represents a valuable alternative to reconstruct long term SLR trends.

4.2. Sediment characterization

Sediments in tropical salt marshes are a mixture of upland runoff, wetland organic production and suspended marine particles that are transported by tides, and settle and accumulate around the plant stems or following microtopography. Thus, sediment grain size distribution might help to identify hydrodynamic changes, and $\delta^{13}C$ variations can help to trace the terrestrial or marine character of the sediments.

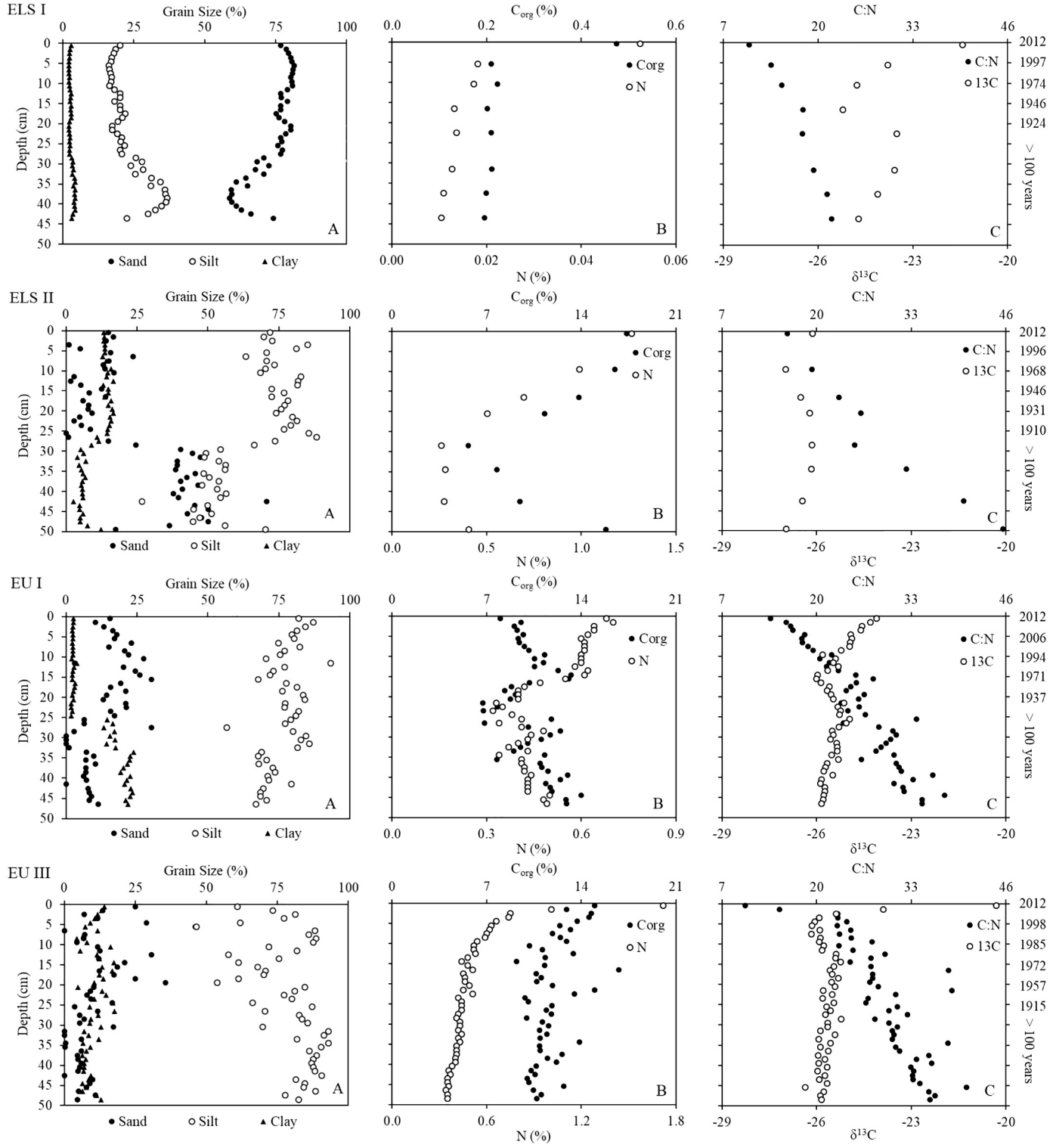

Fig. 3. Characterization of sediment cores from Jiquilisco Bay (ELS) in El Salvador, and from Estero de Urias Lagoon (EU), Salada Lagoon (SA) and Sian Ka'an BR (ISCUL, PUPA) in Mexico. Data from Amaya-Monterrosa et al. (2014), Ruiz-Fernández et al. (2016), Carnero-Bravo et al. (2016), and Bojórquez-Sánchez et al. (2017) except $\delta^{13}C$ and C:N from ELS and SA.

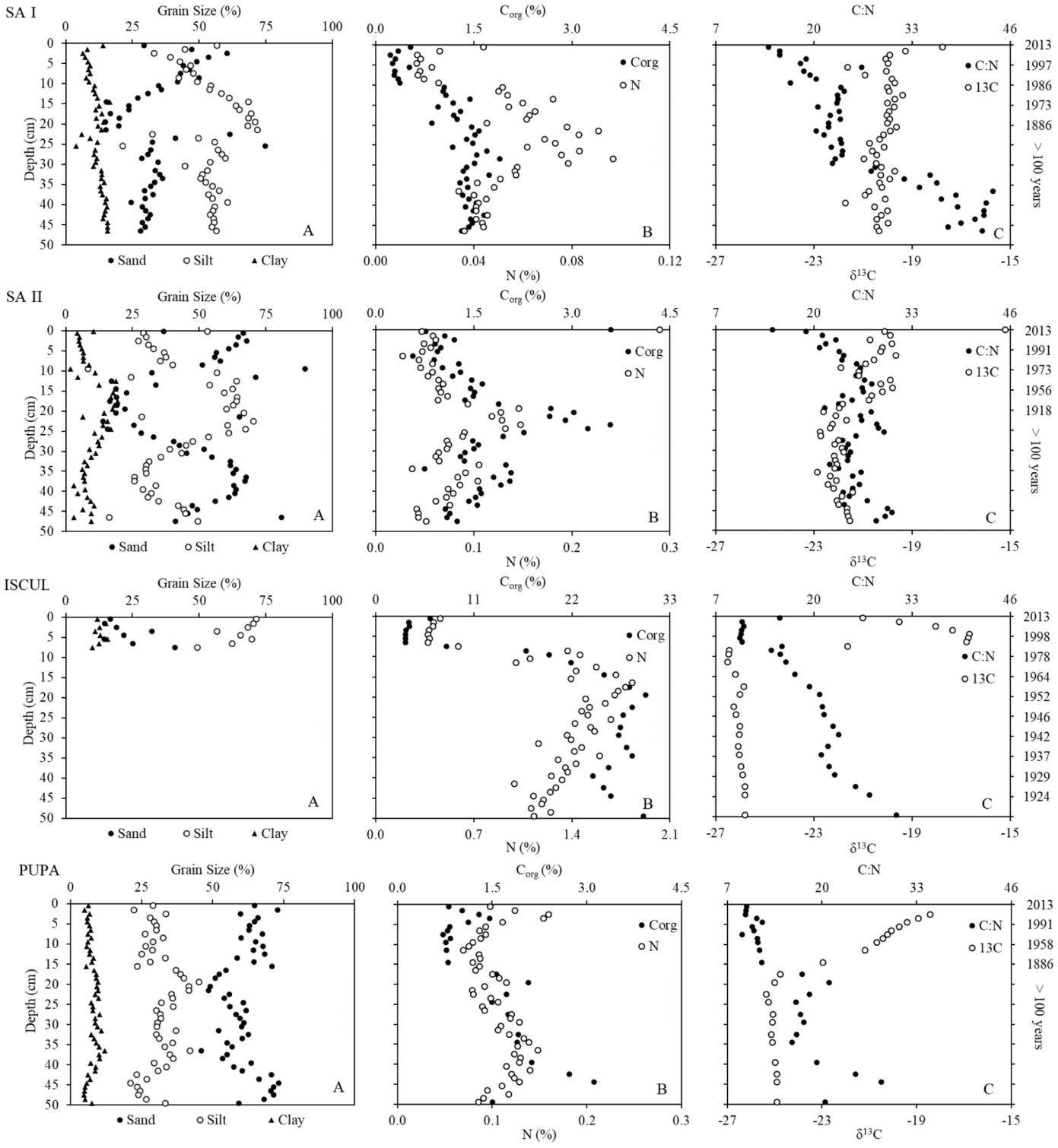

Fig. 3 (*continued*).

4.2.1. Grain size distribution

All cores were composed mainly of sand and silt, with small percentages of clay (<25%). The depth profile of the grain size distribution (Fig. 3) was almost uniform in cores ELS I, EU I, EU III and PUPA; in cores SA I and SA II it showed a cyclic variation between silt and sand content; and in core ELS II it showed a transition from sandy to silty sediments. In Sian Ka'an BR, the deeper segments of both sediment cores contained mangrove remnants (roots and wood chunks) accounting for ~5% of the section mass below 20 cm depth in PUPA, and ~30% below ~10 cm in ISCUL. In fact, mineral material was almost absent from the section of ISCUL enriched by plant debris, so grain size analysis was not feasible.

4.3. Organic carbon

4.3.1. Organic carbon concentrations and trends

C_{org} concentrations ranged from <1% to 30% (Fig. 3). Highest C_{org} concentrations were usually observed in cores with higher contents of

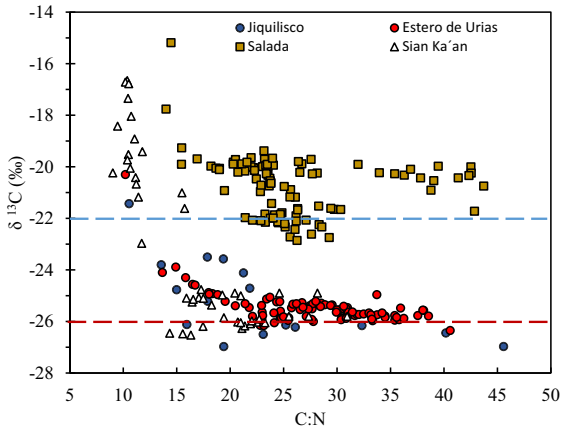

Fig. 4. $\delta^{13}C$ versus C:N distribution in sediment cores from Jiquilisco Bay (El Salvador), and from Estero de Urias Lagoon, Salada Lagoon, and Sian Ka'an Reserve of the Biosphere (Mexico). The discontinuous lines indicate typical $\delta^{13}C$ values for the marine (blue) and terrestrial (red) end members (Gearing et al., 1984). (For interpretation of the references to color in this figure legend, the reader is referred to the web version of this article.)

fine sediment, in agreement with the common observation that fine-grained particles have a larger surface area by unit volume and adsorb C_{org} more efficiently than coarser particles (Loring and Rantala, 1992). However, highest C_{org} concentrations were observed in the section of core ISCUL with high plant debris content (for which there is no information regarding grain size).

None of the depth profiles for C_{org} concentration showed the typical exponential decay trend expected under steady-state conditions of C_{org} accumulation and decomposition (Berner, 1980). In fact, C_{org} concentrations varied little with depth, although in cores ELS I, ELS II, SA II and EU III the highest C_{org} concentrations were observed in the uppermost core segment, whereas in EU I, SA I, PUPA and ISCUL, C_{org} concentrations were higher towards the core bottom (Fig. 3).

4.3.2. Organic carbon provenance

Sources of organic matter are commonly inferred from sediment bulk properties such as elemental composition, C:N ratios and stable isotopes of C and N. Terrestrial organic matter, composed mainly of vascular plant debris, is assumed to have C:N > 20 (Meyers, 1997), $\delta^{13}C$ between −25‰ and −28‰ (Burdige, 2005) and $\delta^{15}N$ around +0.4 ± 0.9‰ (Peterson and Howard, 1987). Marine-derived organic matter is characterized by C:N < 10 (Parsons, 1975), $\delta^{13}C$ from −17‰ to −24‰ (Gearing et al., 1984) and $\delta^{15}N$ between 3‰ and 12‰ (Wada and Hattori, 1990). Thus, organic matter in coastal sediments should present C:N, $\delta^{13}C$ and $\delta^{15}N$ values between the ranges for terrestrial and marine end members. Ranges in our cores (Table 1) clearly show the mixed nature (terrestrial and marine) of organic matter in these sediments.

In all cores, depth profiles showed decreasing C:N ratios and increasing $\delta^{13}C$ values towards the surface (Fig. 3), indicating an increasing supply of marine organic matter (Fig. 4), which support that these low-lying tropical salt marshes are already reflecting marine transgression due to recent sea level rise (Ruiz-Fernández et al., 2016; Carnero-Bravo et al., 2016).

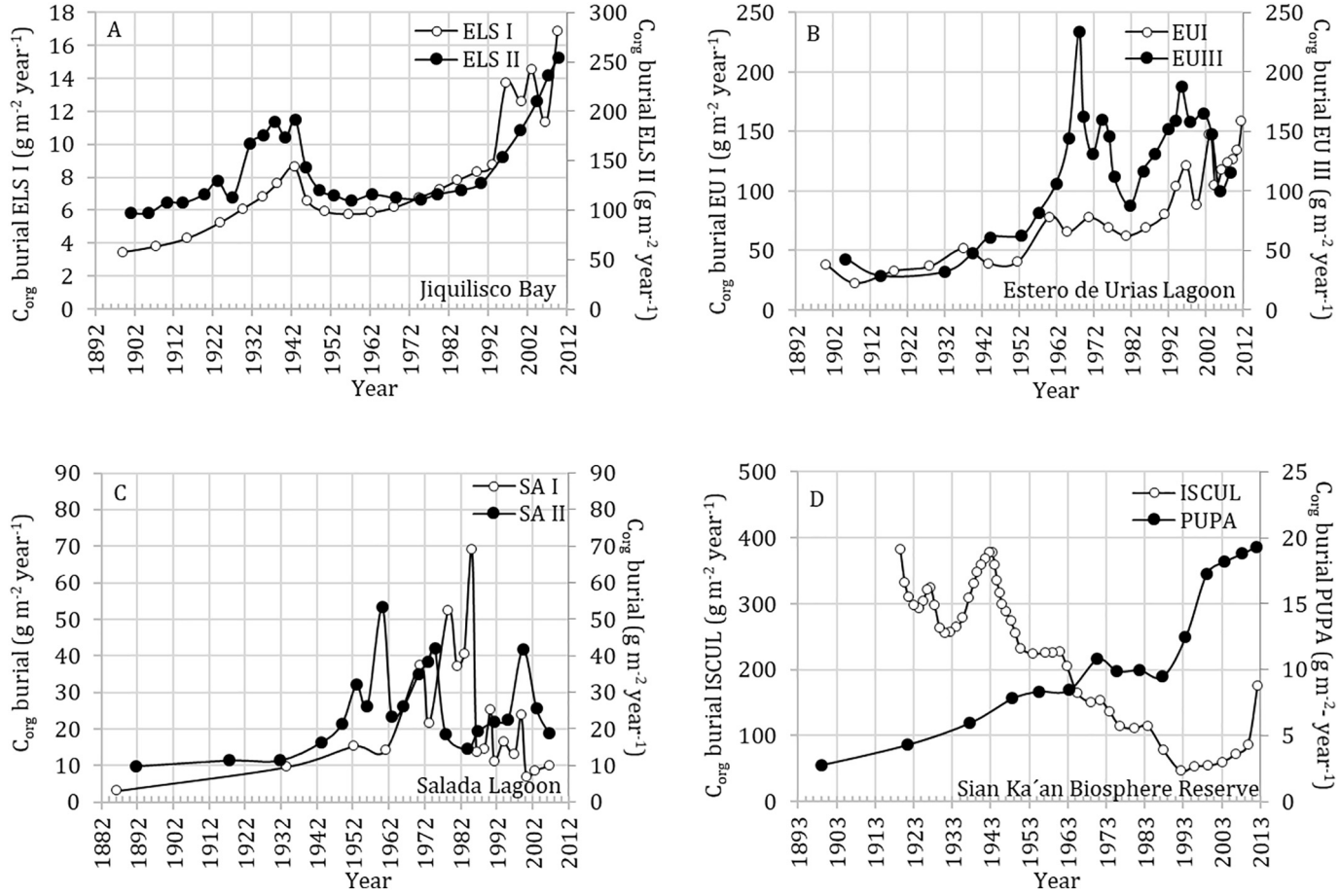

Fig. 5. Time-dependent C_{org} burial rates in sediment cores collected in tropical salt marshes from (A) Jiquilisco Bay (El Salvador), and from (B) Estero de Urias Lagoon, (C) Salada Lagoon, and (D) Sian Ka'an BR (Mexico).

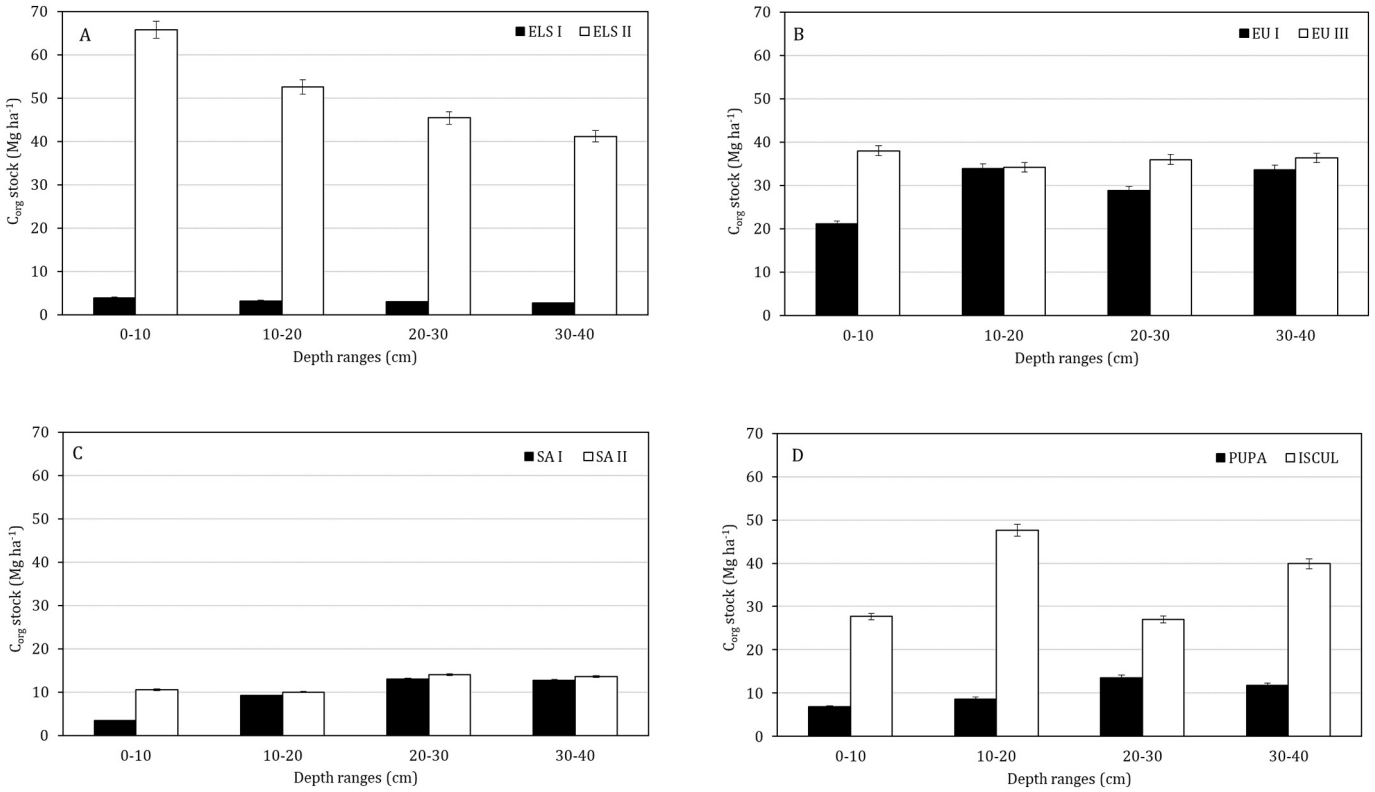

Fig. 6. C_{org} stock (from surface down to 40 cm depth) in sediments from tropical salt marshes at Jiquilisco Bay (A = ELS I and ELS II) in El Salvador, and from Estero de Urias Lagoon (B = EU I and EU III), Salada Lagoon (C = SA I and SA II), and Sian Ka'an BR (D = PUPA, ISCUL).

4.3.3. Organic carbon burial and storage

As none of the depth profiles for C_{org} concentration showed the typical exponential decay caused by microbial degradation, it was impossible to evaluate the effects of diagenesis by using first-order mineralization models (e.g. Berner, 1964; Middelburg, 1989). The C_{org} burial rate (i.e. deposition at the sediment surface) was estimated by multiplying C_{org} concentrations by mass accumulation rates, assuming that C_{org} concentrations represent those accumulated at the surface layer at the time of deposition, as if diagenesis effects were negligible.

C_{org} burial rates ranged from 2.8 ± 0.9 to 378.0 ± 33.8 g m^{-2} year^{-1} (Table 1) and changed considerably within and among the study sites, with highest values in core ISCUL (Sian Ka'an BR), and lowest in the sandy sediments of ELS I (Jiquilisco Bay) and PUPA (Sian Ka'an BR). C_{org} burial rates also changed widely with time, but time-dependent C_{org} burial rate profiles for the two cores at each study site were comparable, excepting for cores PUPA and ISCUL, which showed opposite time-dependent profiles (Fig. 5D). With the exception of core ISCUL, C_{org} burial rates in all cores gradually increased from the 1900s to the 1950s; subsequently, their patterns were diverse, with more abrupt and intermittent changes, particularly in cores from Estero de Urias (EU, Fig. 5B) and Salada (SA, Fig. 5C) lagoons, which are the most anthropized areas among the study sites.

C_{org} stock (i.e. the amount of organic carbon stored per unit area down to a defined sediment depth) was calculated every 10 cm, from surface down to 40 cm depth, as the sum of the product of dry bulk density, C_{org} concentrations and thickness of each core section; the uncertainties of C_{org} stock calculations were estimated by quadratic uncertainty propagation (Fig. 6). The largest and smallest total C_{org} stock values (surface-40 cm depth) were found in cores from a single site (Jiquilisco Bay) with a value ~16-fold larger in ELS II than in ELS I (Table 2). In both cores, the surface (0–10 cm) C_{org} stocks were ~20% higher than in the underlying segment (Fig. 6), reflecting either a slight increase of C_{org} concentrations in the uppermost layer or a small C_{org} degradation with depth. In contrast, in cores EU I, SA I, PUPA and ISCUL, the surface C_{org} stocks were between ~30% and ~60% lower than the segment immediately below, which might be explained by a lower recent C_{org} supply. Except in ISCUL core, the C_{org} stocks in the deepest segments (20–30 cm and 30–40 cm) were very similar, suggesting that below 20 cm C_{org} degradation is negligible. However, in the ISCUL core (Sian Ka'an BR) the C_{org} stock in the deepest segment was almost 40% higher than the overlying one.

Under the assumption of negligible C_{org} degradation with depth, we used the average C_{org} stock of the 20–40 cm depth segments to extrapolate the C_{org} stock to 1 m depth, in order to compare our results with those from studies where the C_{org} stock is calculated following the "blue carbon initiative" methodology (Howard et al., 2014). The C_{org} stock values at 1 m in our sites ranged from 29.9 ± 0.4 to 464.8 ± 6.5 Mg ha^{-1} (Table 2). In addition, taking into account that the time frame was different among the salt marshes owing to differences in mass accumulation rates, the C_{org} stock was also calculated for the past 50 and 100 years (Table 2). At our sites, C_{org} stocks accumulated during the past 50 years usually accounted for more than half of the stock accumulated during the past 100 years, except in ISCUL, where it accounted for only ~25%.

5. Discussion

Considering the diverse environmental settings and anthropization of these study sites, it is remarkable that the sedimentary records were so similar regarding grain size distribution, C:N ratios and $\delta^{13}C$ trends, which implies the occurrence of similar sedimentary and geochemical processes at most sites.

Table 2
C_{org} stock (Mg ha^{-1}) by depth and time, in sediment cores from tropical salt marshes in El Salvador and Mexico.

Core	C_{org} stock by depth (Mg ha^{-1})					C_{org} stock by time (Mg ha^{-1})			CO_{2eq}
	0–10 cm	10–20 cm	20–30 cm	30–40 cm	0–100 cm[a]	50 years	100 years	Stock ratio (%)	Mg CO_2/ha[b]
ELSI	3.9 ± 0.1	3.2 ± 0.1	3.0 ± 0.1	2.7 ± 0.1	29.9 ± 0.5	4.6 ± 0.1	7.5 ± 0.2	62	110 ± 2
ELSII	65.8 ± 2.0	52.6 ± 1.6	45.4 ± 1.4	41.2 ± 1.3	464.8 ± 7.2	72.7 ± 2.1	142.5 ± 2.8	51	1706 ± 24
EUI	21.2 ± 0.7	34.0 ± 1.0	28.9 ± 0.9	33.7 ± 1.0	305.3 ± 4.8	41.5 ± 1.1	63.9 ± 1.3	65	1120 ± 16
EUIII	38.0 ± 1.2	34.3 ± 1.1	36.0 ± 1.1	36.4 ± 1.1	362.0 ± 2.8	68.4 ± 1.5	89.5 ± 1.8	76	1329 ± 18
SAI	3.5 ± 0.1	9.2 ± 0.2	13.0 ± 0.2	12.7 ± 0.2	115.6 ± 1.0	10.2 ± 0.1	11.9 ± 0.2	86	424 ± 4
SAII	10.6 ± 0.2	10.0 ± 0.2	14.0 ± 0.2	13.5 ± 0.2	130.7 ± 1.1	13.2 ± 0.2	20.6 ± 0.2	64	480 ± 4
ISCUL	27.7 ± 0.7	47.6 ± 1.4	27.0 ± 0.8	39.9 ± 1.2	342.8 ± 5.2	48.5 ± 1.1	182.3 ± 2.5	27	1258 ± 18
PUPA	6.8 ± 0.3	8.6 ± 0.5	13.6 ± 0.6	11.8 ± 0.5	116.9 ± 2.8	6.0 ± 0.4	9.6 ± 1.2	63	429 ± 10
Min	3.5 ± 0.1	3.2 ± 0.1	3.0 ± 0.1	2.7 ± 0.1	29.9 ± 0.4	4.6 ± 0.1	7.5 ± 0.2	27	110 ± 2
Max	65.8 ± 2.0	52.6 ± 1.6	45.4 ± 1.4	41.2 ± 1.3	464.8 ± 6.5	72.7 ± 2.1	182.3 ± 2.5	86	1706 ± 24

Min and max = minimum and maximum values, respectively, taking into account all the observations of all sediment cores.
[a] Extrapolated data up to 1 m depth, assuming negligible C_{org} degradation below 40 cm depth (see text).
[b] Equivalent of CO_2 = potential carbon emissions from alteration to the environment based on C_{org} stock at 1 m depth (Howard et al., 2014). Stock ratio = C_{org} stock in 50 years/C_{org} stock in 100 years.

5.1. Energy of the depositional environments

Grain size distribution varied notably along the records ELS II, SA I and SA II (Fig. 3), denoting hydrodynamic changes in the salt marsh environments. In core ELS II, the transition from sandy (below 25 cm depth) to silty sediments (surface to 25 cm depth) occurred >100 years ago, indicating a shift from a higher- to a lower-energy environment, which was attributed to sea level rise, since recent sections contained remains of planktonic foraminifera carried by tidal currents (Amaya-Monterrosa et al., 2014). Rising sea level increases the probability and intensity of flooding low-lying coastal regions, and contributes to the redistribution of sediment along sandy coasts. The attenuation effect of the mangroves on the energy of the waves would promote that coarser particles are retained in the lower reaches of the intertidal zone, while the colonization of former upland areas by salt-resistant vegetation would promote that fine particles carried out by the tides are deposited in new flooded areas, where eventually would develop an onlap sequence, in which coarser sediments are covered by finer ones (Levin and King, 2017). In Salada Lagoon, the low sand content at 10 to 20 cm in core SAI and at 10 to 30 cm in core SAII could be related to periods of desiccation and infilling. There is no information on the timeline and factors that might have promoted such events in the Salada Lagoon in the past, but a similar recent siltation process in a nearby lagoon is attributed to high evaporation caused by the seasonal closure of the lagoon mouth, acting together with the high erodibility of the surrounding terrain during the rainy season (Plata, 2005). The increase in sand content in the uppermost layers of both cores indicated a reversal from infilling conditions to a higher-energy environment between the 1970s and 1980s, caused by the opening of the channel that conducts the cooling waters from the Laguna Verde nuclear power plant to the sea, which keeps the lagoon permanently connected to open sea waters.

In the ISCUL core from Sian Ka'an, the transition from sediments enriched with plant debris (10 to 50 cm depth) to silty grained sediments (surface to 10 cm depth) indicated that the current salt marsh area was formerly a mangrove forest. This transition was likely due to significant changes in environmental conditions (e.g. flooding, erosion, subsidence, soil hypersalinization) that are generally followed by alterations in the vigor or zonation of mangrove trees, which may include widespread tree mortality (Jimenez et al., 1985). At the Sian Ka'an BR ISCUL station, a probable reason for this change may have been hypersalinization caused by sea level rise.

5.2. C_{org} concentrations, burial rate and stock

The departure from exponential decay trends in most of the C_{org} depth profiles (Fig. 3B) could be indicative of non-steady C_{org} supply or non-steady degradation. However, taking into account the variations in sediment grain size distribution and in the provenance of the sediments (recent marine transgression) we considered that variations in C_{org} inputs are the most plausible explanation for these profiles. Non-steady-state conditions may be fostered by a combination of factors, such as tidal advection and temporal changes in supply rates and quality of organic sedimentation (Alongi et al., 1996). The almost constant C_{org} concentrations in some core segments (e.g. in ELS I, EU I, EU III and ISCUL; Fig. 3B) could indicate mixing or the presence of slump deposits, but these were ruled out since ^{210}Pb profiles should also be flat, which was not the case (Fig. 2). Furthermore, C_{org} decay after burial was apparently almost negligible in most cases. Indeed, aerobic degradation of labile organic material near the surface of organic-rich sediments is usually so rapid that oxygen rarely penetrates >2 mm into the sediment, therefore limiting C_{org} degradation (Kristensen et al., 2008).

Wetland C_{org} decay rates vary in relation with climate (temperature and moisture) and the quality (chemical composition) of the organic matter entering the system (Schlesinger, 1997). Organic matter derived from vascular plants, such as marsh plants, mangroves and seagrasses (Moran and Hodson, 1989) is enriched in ligneous and phenolic compounds, which are refractory and require microbial breakdown to convert the more recalcitrant polymers to the more labile C_{org} available to consumers. Low oxygen concentrations in the sediment (i.e. reduced conditions) and high sediment accretion rates may also reduce C_{org} decay (Müller and Suess, 1979). In the upper core segments, where more marine conditions were identified, sediments accumulated allochthonous marine organic matter, including refractory organic matter transported from elsewhere; high concentrations of suspended particulate matter and repeated cycles of sedimentation and resuspension over diurnal and neap-spring tidal cycles promote high rates of organic matter remineralization within these zones (Abril et al., 1999).

Both cores in Sian Ka'an RB, as well as at least one of the cores in the other three study sites (ELS II in Jiquilisco Bay; EU I in Estero de Urias Lagoon, and SA I in Salada Lagoon) showed decreasing C_{org} concentrations with increasing $\delta^{13}C$ values (more marine conditions; Fig. 7). The overall assessment of the data set provided a significant inverse correlation ($p < 0.05$) suggesting a negative impact of marine transgression on C_{org} concentrations. Indeed, other studies suggest that C_{org} sequestration in coastal environments is likely to decline with sea level rise (Van de Broek et al., 2016), mostly due to the reduction of terrestrial organic matter supply. However, it could be also due to a higher input of inorganic particles, such as clastic material from sediment resuspension, or biological remains such as the silica frustules of diatoms or the calcium carbonate shells of coccolithophorids. In addition, flooding may enhance organic matter decay rates even in water-logged soils (Kirwan et al., 2013) and salinity increases C_{org} microbial decomposition rates in tidal wetland sediments (Morrissey et al., 2014).

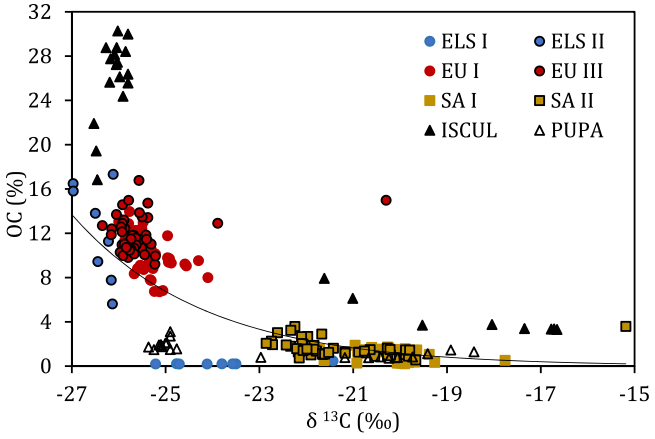

Fig. 7. C_{org} concentrations and $\delta^{13}C$ distribution in sediment cores from Jiquilisco Bay (ELS), the Estero de Urias Lagoon (EU), Salada Lagoon (SA), and Sian Ka'an BR (ISCUL, PUPA). The correlation coefficient ($r = 0.73$) is significant (Student's *t*-test, $p < 0.05$).

C_{org} burial rates (Table 1) and C_{org} stocks (Table 2) showed very different values among and within the study sites, which highlights the complex diversity nature of tropical salt marshes. In fact, both the minimum and maximum values of C_{org} burial rates and C_{org} stocks (at 1 m) were found in Sian Ka'an (Table 1) and Jiquilisco Bay (Table 2), respectively. C_{org} burial rates, highly variable in these tropical salt marshes, can reach considerably higher rates than those of peatlands from the northern hemisphere, and are comparable to the ranges reported for mangrove and salt marsh areas around the world (Table 3).

Most cores in the present study (except ISCUL, Sian Ka'an BR) showed steadily increasing C_{org} burial rates between the 1900s and 1950s; more abrupt and intermittent changes followed, and finally increases (except SAI and SAII cores from Salada Lagoon, Fig. 5). Since in most cores the C_{org} concentration depth profiles did not show significant increases associated with marine transgression (Fig. 3), we consider that C_{org} burial rates in our study sites are strongly influenced by changes in mass accumulation rates, which could be related to the impact of sea level rise, but also be affected by human interventions. For instance, as already noted (Amaya-Monterrosa et al., 2014) an abrupt decrease in MAR in the early 1950s in the cores of Jiquilisco Bay was related to the construction of dams along the Lempa River, and more recently the increase in MAR might be related to sea-level rise, but also of greater erosion in the drainage basin related to changes in land use and agricultural activities. In Salada Lagoon, the lower C_{org} burial rates since the middle 1980s might appear to be attributable to increasing marine conditions; however, this decrease might be also influenced by the higher-energy conditions caused by the construction of the channel for the cooling waters from the nuclear power plant, which reduced lagoon infilling, and therefore MARs.

C_{org} stock range (10–164 Mg ha^{-1} in the upper 30 cm) was comparable to C_{org} stocks (30 cm depth) for mangrove (57 ± 6 Mg ha^{-1}) and salt marsh (49 ± 5 Mg ha^{-1}) areas in Florida, for which the authors report no significant differences (Doughty et al., 2016). In addition, most C_{org} stocks (1 m depth, extrapolated; Table 2) were i) comparable to 355 Mg ha^{-1} in Delaware Bay salt marshes (O'Hara et al., 2016), ii) within the range for mangrove sites in marine (271–572 Mg ha^{-1}) and estuarine (100–315 Mg ha^{-1}) areas in Indonesia (Weiss et al., 2016), and iii) similar to freshwater mangroves (101–491 Mg ha^{-1}) on the Mexican coast of the Gulf of Mexico (Kauffman et al., 2016). All these results confirm the importance of mangrove and tropical salt marsh sediments as C_{org} reservoirs, in either freshwater or coastal environments. The potential CO_2 emissions resulting from a given change in land use were calculated by multiplying C_{org} stocks by 3.67, the molecular weight ratio of CO_2 to C (Pendleton et al., 2012); for the C_{org} stocks determined in the present study, they varied from 110 to 1706 Mg of potential CO_2 emissions per hectare.

Table 3
C_{org} burial rates for wetlands worldwide.

Study site	C_{org} burial rate (g m^{-2} $year^{-1}$)	Reference
Mangroves		
Global mean	100	Twilley et al., 1992
Global mean	174 ± 23	Alongi, 2014
Estimated global value	167	Alongi, 2012
Estimated global value (geometric mean)	139	Duarte et al., 2005
Mean value from Gulf of Mexico, Pacific and Indian Ocean	188 ± 142[a]	Chmura et al., 2003
Revision of global burial rate	115[a]	Bouillon et al., 2008
Global geometric mean at the local scale[b]	163 (+40, −31)	Breithaupt et al., 2012
Riverine area (past 50 years)	162 ± 5	Marchio et al., 2016
Fringe area (past 50 years)	127 ± 6	Marchio et al., 2016
Everglades National Park	151–168	Smoak et al., 2013
Salt marshes		
Estimated global value (geometric mean)	151	Duarte et al., 2005
Northern hemisphere mean value	218 ± 235[a]	Chmura et al., 2003
Mean value ($n = 96$ sites)	218 ± 24	Mcleod et al., 2011
Peatlands		
Boreal areas	29 ± 13	Mitsch et al., 2013
Canada	20–30	Roulet, 2000
Europe and North American boreal areas	23	Dean and Gorham, 1998
Finland boreal areas	26	Turunen et al., 2002
Finland Arctic areas	17	Turunen et al., 2002
Scottish inundated areas	42	Whittle and Gallego-Sala, 2016
Tropical salt marshes		
Jiquilisco Bay, El Salvador	3–255	This study
Estero de Urias Lagoon, Mexico	22–234	This study
Salada Lagoon, Mexico	3–94	This study
Sian Ka'an Biosphere Reserve, Mexico	3–383	This study

[a] Calculated from the original reference.
[b] Confidence interval (95%).

Our results show that C_{org} storage varies considerably within a single type of environment, and also with time. In general, salt marsh carbon storage depends upon a balance between carbon inputs and decomposition (Kirwan and Blum, 2011), and on local wetland conditions such as hydrology (Doughty et al., 2016). Thus, a reliable quantification of C_{org} stocks requires a good understanding of i) the tropical salt marsh settings, including the energy of the environment and, consequently, the grain size of the sediments, and ii) the impacts of human interventions.

These results indicate that enhanced marine conditions caused by sea level rise promoted lower C_{org} sediment concentrations, but increased C_{org} burial rates, although these can also be strongly influenced by changes of sediment accretion rates caused by anthropogenic impacts. According to Figueiredo et al. (2014), the relationship between sea level rise and sediment accretion rates might be masked by local changes such as deforestation, expansion of farming land, dredging of channels, and increased paving of roadways; this is compatible with the finding by Mariotti and Fagherazzi (2013) that sediment starvation produced by river dredging and damming is a major anthropogenic driver of marsh loss and generates effects at least comparable to the accelerating sea-level rise due to global warming.

6. Conclusions

^{210}Pb-dated sediment cores collected from tropical salt marshes in coastal areas of Mexico and El Salvador, already described separately in published reports, were here analyzed to evaluate the temporal

variations of C_{org} concentrations, burial rates and stocks, under the influence of sea level rise. C_{org} burial rates and C_{org} stocks varied widely between and among the study areas; the lowest and higher values observed among all the cores were 3 and 378 g m^{-2} $year^{-1}$, and 30 and 465 Mg ha^{-1}, respectively; these values fell within the ranges reported for coastal wetland areas worldwide. Our results confirmed that tropical salt marshes are areas of high C_{org} accumulation, and that C_{org} decomposition within the sediments is small. In general, marine transgression was associated to lower C_{org} sediment concentrations, likely caused by the accumulation of refractory sedimentary C_{org} transported by tidal currents and dilution by a higher input of inorganic particles. In addition, C_{org} burial rates can be significantly influenced by changes in mass accumulation rates induced by increasing tidal flooding, but also by human interventions (e.g. higher MAR owing to erosion from the catchment as a result of land use changes, or lower MAR due to retention of sediments promoted by dam construction). We conclude that, although C_{org} storage in tropical salt marshes is substantial, it can be reduced by global climate change; this emphasizes the importance of protecting these environments to preserve their capacity to mitigate global warming.

Acknowledgements

Financial support was provided through the grants CONACYT 2010/153492, CONACYT PDCPN 2015-1-473, CONACYT PDCPN 2013-01/214349 and the PRODEP network "Aquatic contamination: levels and effects" (year 3). Thanks are due to the support of the Laboratory of Environmental Engineering of the Nuclear Power Plant Laguna Verde, as well as to A. Galaviz-Solís, S. Rendón-Rodríguez, J.A. Reda Deara, H. Álvarez Guillén, M. A. Gómez-Ponce, during sampling work; and to G. Ramírez, C. Suárez and D. Oviedo for technical assistance. Fellowships for postgraduate studies of SBS, VCB and PGLM were provided by CONACYT. The authors are indebted to Ann Grant for the grammar and style review of this article.

Appendix A. Supplementary data

Supplementary data to this article can be found online at https://doi.org/10.1016/j.scitotenv.2018.02.246.

References

Ablain, M., Legeais, J.F., Prandi, P., Marcos, M., Fenoglio-Marc, L., Dien, H.B., Benveniste, J., Cazenave, A., 2017. Satellite altimetry-based sea level at global and regional scales. Surv. Geophys. 38, 7–31.

Abril, G., Etcheber, H., Le Hir, P., Bassoullet, P., Boutier, B., Frankignoulle, M., 1999. Oxic/anoxic oscillations and organic carbon mineralization in an estuarine maximum turbidity zone (The Gironde, France). Limnol. Oceanogr. 44 (5), 1304–1315.

Alba-Cornejo, V.M., Machado-Navarro, A., González-Millán, J., Herrera-Santoyo, C., Ledesma-Vázquez, J., Rico-Domínguez, R., Vera-Morán, A., 1979. Estudio sedimentológico de la bahía de Puerto Viejo, Mazatlán, Sinaloa. An. Inst. Cien. Mar Limnol. UNAM México 6 (1), 97–120.

Alongi, D.M., 2012. Carbon sequestration in mangrove forests. Carbon Manag. 3 (3), 313–322.

Alongi, D.M., 2014. Carbon cycling and storage in mangrove forests. Annu. Rev. Mar. Sci. 6, 195–219.

Alongi, D.M., Brinkman, R., 2011. Hydrology and biogeochemistry of mangrove forests. In: Levia, D.F., Carlyle-Moses, D., Tanaka, T. (Eds.), Forest Hydrology and Biogeochemistry vol. 216. Springer Netherlands, pp. 203–219.

Alongi, D.M., Tirendi, F., Goldrick, A., 1996. Organic matter oxidation and sediment chemistry in mixed terrigenous-carbonate sands of Ningaloo Reef, Western Australia. Mar. Chem. 54 (3–4), 203–219.

Amaya-Monterrosa, O.A., Machain-Castillo, M.L., Ruiz-Fernández, A.C., Sanchez-Cabeza, J.A., Carranza-Edwards, A., Cearreta, A., Rodríguez-Ramírez, A., 2014. Evidencias geoquímicas y micropaleontológicas de cambios hidrológicos recientes en registros sedimentarios de la bahía de Jiquilisco, El Salvador. Ciencias marinas 40 (4), 305–320.

Berner, R.A., 1964. An idealized model of dissolved sulfate distribution in recent sediments. Geochim. Cosmochim. Acta 28 (1964), 1497–1503.

Berner, R.A., 1980. Early Diagenesis: A Theoretical Approach. Princeton University Press, Princeton, USA (245 pp).

Bojórquez-Sánchez, S., Marmolejo-Rodríguez, A.J., Ruiz-Fernández, A.C., Sánchez-González, A., Sánchez-Cabeza, J.A., Bojórquez-Leyva, H., Pérez-Bernal, L.H., 2017. Trace element fluxes during the last 100 years in sediment near a nuclear power plant. Estuar. Coast. Shelf Sci. 198 (Part B), 343–353.

Bouillon, S., Borges, A.V., Castañeda-Moya, E., Diele, K., Dittmar, T., Duke, N.C., ... Rivera-Monroy, V.H., 2008. Mangrove production and carbon sinks: a revision of global budget estimates. Glob. Biogeochem. Cycles 22 (2).

Breithaupt, J.L., Smoak, J.M., Smith, T.J., Sanders, C.J., Hoare, A., 2012. Organic carbon burial rates in mangrove sediments: strengthening the global budget. Glob. Biogeochem. Cycles 26 (3), 1–11 (GB3011).

Burdige, D.J., 2005. Burial of terrestrial organic matter in marine sediments: a re-assessment. Glob. Biogeochem. Cycles 19 (4), 1–7 (GB4011).

Cardoso-Mohedano, J.G., Bernardello, R., Sanchez-Cabeza, J.A., Molino-Minero-Re, E., Ruiz-Fernández, A.C., Cruzado, A., 2015. Accumulation of conservative substances in a subtropical coastal lagoon. Estuar. Coast. Shelf Sci. 164, 1–9.

Carnero-Bravo, V., Sanchez-Cabeza, J.A., Ruiz-Fernández, A.C., Merino-Ibarra, M., Hillaire-Marcel, C., Corcho-Alvarado, J.A., Zavala-Hidalgo, J., 2016. Sedimentary records of recent sea level rise and acceleration in the Yucatan Peninsula. Sci. Total Environ. 573, 1063–1069.

Chmura, G.L., Anisfeld, S.C., Cahoon, D.R., Lynch, J.C., 2003. Global carbon sequestration in tidal, saline wetland soils. Glob. Biogeochem. Cycles 17 (4), 1–12.

CONABIO, 2012. Comisión Nacional para el Conocimiento y Uso de la Biodiversidad. http://www.conabio.gob.mx/conocimiento/regionalizacion/doctos/Mlistado.html.

CO-OPS-NOS-NOAA, 2013. Sea level trends. Center for Operational Oceanographic Products and Services, National Ocean Service, National Oceanographic Atmospheric Administrationhttps://tidesandcurrents.noaa.gov/sltrends/sltrends.html, Accessed date: 18 February 2018.

Costa, C.S., Iribarne, O.O., Farina, J.M., 2009. Human impacts and threats to the conservation of South American salt marshes. In: Silliman, B.R., Grosholz, E.D., Bertness, M.D. (Eds.), Human Impacts on Salt Marshes: A Global Perspective. University of California Press, Berkeley, CA, pp. 337–360.

Dean, W.E., Gorham, E., 1998. Magnitude and significance of carbon burial in lakes, reservoirs, and peatlands. Geology 26 (6), 535–538.

Doughty, C.L., Langley, J.A., Walker, W.S., Feller, I.C., Schaub, R., Chapman, S.K., 2016. Mangrove range expansion rapidly increases coastal wetland carbon storage. Estuar. Coasts 39 (2), 385–396.

Duarte, C.M., Middelburg, J.J., Caraco, N., 2005. Major role of marine vegetation on the oceanic carbon cycle. Biogeosciences 2 (1), 1–8.

Figueiredo, A.G., de Toledo, M.B., Cordeiro, R.C., Godoy, J.M., da Silva, F.T., Vasconcelos, S.C., y dos Santos, R.A., 2014. Linked variations in sediment accumulation rates and sea-level in Guanabara Bay, Brazil, over the last 6000 years. Palaeogeogr. Palaeoclimatol. Palaeoecol. 415, 83–90.

Flores-Verdugo, F.J., Agraz-Hernández, C., Benitez-Pardo, D., 2007. Ecosistemas acuáticos costeros: Importancia, retos y prioridades para su conservación. In: Sánchez, O., Herzig, M., Peters, E., et al. (Eds.), Perspectivas sobre conservación de ecosistemas acuáticos en México. Secretaria de Medio Ambiente y Recursos Naturales. Instituto Nacional de Ecología, México, pp. 145–147.

Gearing, J.N., Gearing, P.J., Rudnick, D.T., Requejo, A.G., Hutchins, M.J., 1984. Isotopic variability of organic carbon in a phytoplankton-based, temperate estuary. Geochim. Cosmochim. Acta 48 (5), 1089–1098.

Gonneea, M.E., Paytan, A., Herrera-Silveira, J.A., 2004. Tracing organic matter sources and carbon burial in mangrove sediments over the past 160 years. Estuar. Coast. Shelf Sci. 61 (2), 211–227.

Hay, C.C., Morrow, E., Kopp, R.E., Mitrovica, J.X., 2015. Probabilistic reanalysis of twentieth-century sea-level rise. Nature 517, 481–484.

Howard, J., Hoyt, S., Isensee, K., Pidgeon, E., Telszewski, M. (Eds.), 2014. Coastal Blue Carbon: Methods for Assessing Carbon Stocks and Emissions Factors in Mangroves, Tidal Salt Marshes and Seagrass Meadows. Conservation International, Intergovernmental Oceanographic Commission of UNESCO, International Union for Conservation of Nature, Arlington, USA (180 pp).

INEGI, 2009. Prontuario de informacion geográfica municipal de los Estados Unidos Mexicanos.Available at:. http://www3.inegi.org.mx/sistemas/mexicocifras/datosgeograficos/25/25012.pdf (Mazatlán, Sinaloa).

Jimenez, J.A., Lugo, A.E., Cintron, G., 1985. Tree mortality in mangrove forests. Biotropica 177–185.

Kauffman, J.B., Trejo, H.H., Garcia, M.D.C.J., Heider, C., Contreras, W.M., 2016. Carbon stocks of mangroves and losses arising from their conversion to cattle pastures in the Pantanos de Centla, Mexico. Wetl. Ecol. Manag. 24 (2), 203–216.

Kirwan, M.L., Blum, L.K., 2011. Enhanced decomposition offsets enhanced productivity and soil carbon accumulation in coastal wetlands responding to climate change. Biogeosciences 8 (4), 987.

Kirwan, M.L., Mudd, S.M., 2012. Response of salt-marsh carbon accumulation to climate change. Nature 489, 550–553.

Kirwan, M.L., Langley, J.A., Guntenspergen, G.R., Megonigal, J.P., 2013. The impact of sea-level rise on organic matter decay rates in Chesapeake Bay brackish tidal marshes. Biogeosciences 10 (3), 1869–1876.

Kristensen, E., Bouillon, S., Dittmar, T., Marchand, C., 2008. Organic carbon dynamics in mangrove ecosystems: a review. Aquat. Bot. 89 (2), 201–219.

Levin, H.L., King, D.T., 2017. The Earth Through Time. 11th edition. John Wiley & Sons, Inc., USA (600 pp).

Lynch, J.C., Meriwether, J.R, McKee, B.A., Vera-Herrera, F., Twilley, R.R, 1989. Recent accretion in mangrove ecosystems based on 137Cs and 210Pb. Estuaries 12 (4), 284–299.

Loring, H.D., Rantala, R., 1992. Manual for the geochemical analyses of marine sediments and suspended particulate matter. Earth Sci. Rev. 32, 235–283.

Marchio, D.A., Savarese, M., Bovard, B., Mitsch, W.J., 2016. Carbon sequestration and sedimentation in mangrove swamps influenced by hydrogeomorphic conditions and urbanization in Southwest Florida. Forests 7 (6), 116.

Mariotti, G., Fagherazzi, S., 2013. Critical width of tidal flats triggers marsh collapse in the absence of sea-level rise. Proc. Natl. Acad. Sci. 110 (14), 5353–5356.
MARN, 2013. Geología de El Salvador. Ministerio de Medio Ambiente y Recursos Naturales http://www.snet.gob.sv/ver/geologia/geologia+de+el+salvador/.
MARN/AECI, 2004. Sitio Ramsar Complejo Bahía de Jiquilisco. Ministerio de Medio Ambiente y Recursos Naturales/Agencia Española de Cooperación Internacional http://www.marn.sv/temas/biodiversidad/humedales/bahia-dejiquilisco.html.
Mcleod, E., Chmura, G.L., Bouillon, S., Salm, R., Björk, M., Duarte, C.M., Silliman, B.R., 2011. A blueprint for blue carbon: toward an improved understanding of the role of vegetated coastal habitats in sequestering CO2. Front. Ecol. Environ. 9 (10), 552–560.
Mcowen, C., Weatherdon, L., Bochove, J., Sullivan, E., Blyth, S., Zockler, C., Stanwell-Smith, D., Kingston, N., Martin, C., Spalding, M., Fletcher, S., 2017. A global map of saltmarshes. Biodivers. Data J. 5, e11764.
Meyers, P.A., 1997. Organic geochemical proxies of paleoceanographic, paleolimnologic, and paleoclimatic processes. Org. Geochem. 27 (5), 213–250.
Middelburg, J.J., 1989. A simple rate model for organic matter decomposition in marine sediments. Geochim. Cosmochim. Acta 53 (7), 1577–1581.
Mitsch, W.J., Bernal, B., Nahlik, A.M., Mander, Ü., Zhang, L., Anderson, C.J., Brix, H., 2013. Wetlands, carbon, and climate change. Landsc. Ecol. 28 (4), 583–597.
Moran, M.A., Hodson, R.E., 1989. Formation and bacterial utilization of dissolved organic carbon derived from detrital lignocellulose. Limnol. Oceanogr. 34 (6), 1034–1047.
Morrissey, E.M., Gillespie, J.L., Morina, J.C., Franklin, R.B., 2014. Salinity affects microbial activity and soil organic matter content in tidal wetlands. Glob. Chang. Biol. 20 (4), 1351–1362.
Müller, P.J., Suess, E., 1979. Productivity, sedimentation rate, and sedimentary organic matter in the oceans—I. Organic carbon preservation. Deep Sea Res. Part A 26 (12), 1347–1362.
Nerem, R.S., Beckley, B.D., Fasullo, J.T., Hamlington, B.D., Masters, D., Mitchum, G.T., 2018. Climate-change–driven accelerated sea-level rise detected in the altimeter era. Proc. Natl. Acad. Sci. https://doi.org/10.1073/pnas.1717312115.
O'Hara, B., Nikitina, D., Serzega, M.D., Jennings, D., Scelfo, D., Esrey, S., 2016. Carbon stock and accumulation rates in the Delaware Bay tidal salt marshes. GSA Annual Meeting in Denver, Colorado, USA – 2016 Paper No. 239–3.
Pendleton, L., Donato, D.C., Murray, B.C., Crooks, S., Jenkins, W.A., Sifleet, S., Megonigal, P., 2012. Estimating global "blue carbon" emissions from conversion and degradation of vegetated coastal ecosystems. PLoS One 7 (9), e43542.
Plata, J.C., 2005. Buscan universitarios detener el azolvamiento de la laguna El Llano. Gaceta Universidad Veracruzana. Octubre-diciembre 2005. Nueva época 94–96.Available at:. https://www.uv.mx/gaceta/Gaceta%2094-96/94-96/CAMPUS/CAMPUS_003.htm (in Spanish).
Robbins, J.A., 1978. Geochemical and geophysical applications of radioactive lead isotopes. In: Nriagu, J.O. (Ed.), Biochemistry of Lead. Elsevier, Amsterdam, pp. 85–393.
Rodríguez Castañeda, P.C., 1994. Evaluación de metales en sedimentos, agua y biota de las lagunas Salada, El Llano y La Mancha, Veracruz, México. Facultad de Ciencias, Universidad Nacional Autónoma de México DF (Tesis de Licenciatura, 99 pp, in Spanish).
Roulet, N.T., 2000. Peatlands, carbon storage, greenhouse gases, and the Kyoto protocol: prospects and significance for Canada. Wetlands 20 (4), 605–615.
Ruiz-Fernández, A.C., Hillaire-Marcel, C., 2009. ^{210}Pb-derived ages for the reconstruction of terrestrial contaminant history into the Mexican Pacific coast: potential and limitations. Mar. Pollut. Bull. 59 (4), 134–145.
Ruiz-Fernández, A.C., Sanchez-Cabeza, J.A., Serrato de la Peña, J.L., Perez-Bernal, L.H., Cearreta, A., Flores-Verdugo, F., Dunbar, R., 2016. Accretion rates in coastal wetlands of the southeastern Gulf of California and their relationship with sea-level rise. The Holocene 26 (7), 1126–1137.
Ruiz-Fernández, A.C., Agraz-Hernández, C.M., Sanchez-Cabeza, J.A., Díaz-Asencio, M., Pérez-Bernal, L.H., Chan Keb, C.A., López-Mendoza, P.G., Blanco y Correa, J.M., Ontiveros-Cuadras, J.F., Osti-Saenz, J., Reyes-Castellano, J.E., 2018. Sediment geochemistry, accumulation rates and forest structure in a large tropical mangrove ecosystem. Wetlands https://doi.org/10.1007/s13157-017-0969-2 (submitted).
Sanchez-Cabeza, J.A., Ruiz-Fernández, A.C., 2012. ^{210}Pb sediment radiochronology: an integrated formulation and classification of dating models. Geochim. Cosmochim. Acta 82, 183–200.
Sanchez-Cabeza, J.A., Ruiz-Fernández, A.C., Ontiveros-Cuadras, J.F., Bernal, L.H.P., Olid, C., 2014. Monte Carlo uncertainty calculation of ^{210}Pb chronologies and accumulation rates of sediments and peat bogs. Quat. Geochronol. 23, 80–93.
Schlesinger, W.H., 1997. Biogeochemistry: An Analysis of Global Change. 2nd ed. Academic Press, San Diego, California.
Scholz, M., 2010. Wetland Systems: Storm Water Management Control. Springer Science & Business Media, Manchester (235 pp).
Smoak, J.M., Breithaupt, J.L., Smith, T.J., Sanders, C.J., 2013. Sediment accretion and organic carbon burial relative to sea-level rise and storm events in two mangrove forests in Everglades National Park. Catena 104, 58–66.
Turunen, J., Tomppo, E., Tolonen, K., Reinikainen, A., 2002. Estimating carbon accumulation rates of undrained mires in Finland–application to boreal and subarctic regions. The Holocene 12 (1), 69–80.
Twilley, R.R., Chen, R.H., Hargis, T., 1992. Carbon sinks in mangroves and their implications to carbon budget of tropical coastal ecosystems. Water Air Soil Pollut. 64 (1), 265–288.
Van de Broek, M., Temmerman, S., Merckx, R., Govers, G., 2016. Controls on soil organic carbon stocks in tidal marshes along an estuarine salinity gradient. Biogeosciences 13 (24), 6611–6624.
Wada, E., Hattori, A., 1990. Nitrogen in the Sea: Forms, Abundance, and Rate Processes. CRC press, Boca Raton, FL (213 pp).
Weiss, C., Weiss, J., Boy, J., Iskandar, I., Mikutta, R., Guggenberger, G., 2016. Soil organic carbon stocks in estuarine and marine mangrove ecosystems are driven by nutrient colimitation of P and N. Ecology and evolution 6 (14), 5043–5056.
Whittle, A., Gallego-Sala, A.V., 2016. Vulnerability of the peatland carbon sink to sea-level rise. Sci. Rep. 6, 28758.